Deliverable D 2.3
Full database with thermal material properties and publication of some results

Document type	**Deliverable D 2.3**
Document Version / Status	**1.3**
Primary Authors	**Marc Huger,** marc.huger@unilim.fr, **UNILIM**
Distribution Level	**PU (Public)**
Project Acronym	**ATHOR**
Project Title	**Advanced THermomechanical multiscale mOdelling of Refractory linings**
Grant Agreement Number	**764987**
Project Website	www.etn-athor.eu
Project Coordinator	**Marc Huger,** marc.huger@unilim.fr, **UNILIM**
Document Contributors	**Marc Huger,** marc.huger@unilim.fr, **UNILIM** **Diana Vitiello,** diana.vitiello@unilim.fr, **UNILIM** **Ilona Kieliba,** kieliba@ghi.rwth-aachen.de, **RWTH** **Robert Kaczmarek,** robert.kaczmarek@unilim.fr, **UNILIM**

History of Changes

Version	Date	Author (Organization)	Change	Page
1.0	25.09.2020	Diana Vitiello (UNILIM) Ilona Kieliba (RWTH) Robert Kaczmarek ((UNILIM)	Creation of the first version	All
1.1	26.02.2021	Glyn Derrick (UNILIM), Marc Huger (UNILIM)	Corrections	All
1.2	26.03.2021	Diana Vitiello (UNILIM) Ilona Kieliba (RWTH) Robert Kaczmarek ((UNILIM) Glyn Derrick (UNILIM)	Corrections	All
1.3	20.04.2021	Diana Vitiello (UNILIM) Ilona Kieliba (RWTH)	Final corrections	6-12

European Commission
Horizon 2020
European Union funding
for Research & Innovation

TABLE OF CONTENTS

1 Introduction

Thermal properties are important input parameters that drive thermomechanical behaviour of refractory linings in application. Specific heat, thermal conductivity and thermal expansion are thus three thermal properties essential for thermomechanical modelling in WP3. The present deliverable is dedicated to the description of these properties (specific output of Task 2.3). The values of these properties in-fact vary with both temperature and the evolution of the microstructure. In other words, the behaviour in service conditions and at room temperature is not necessarily the same and, in addition, room temperature values could be affected by heating cycles. Since refractory materials work at very high temperatures, it is thus fundamental to study the evolution of the thermal properties with temperature.

This deliverable will review the measurements obtained, on the studied materials, for; i) coefficient of thermal expansion (CTE), ii) heat capacity (Cp) and iii) thermal conductivity (λ). The measurement of CTE in the temperature range 20 °C to 1500 °C is a rather standard procedure, the access to accurate values of Cp and λ, however, are still a challenging topic. The Deliverable 1.3 has already detailed different aspects regarding experimental devices which can be used for the measurement of CTE, Cp and λ. The present deliverable aims to (a) establish the best practice for thermal properties measurement on refractory materials and (b) characterize Cp and λ on selected commercial refractories and model materials for numerical modelling.

This document is divided in two main parts. The first part will summarise the results for the materials investigated in the ATHOR project. The values will be summarized in a table as a “Full Database of Thermal Properties”. The second part will be dedicated to a short reminder about the techniques which have been used, with a focus on some points that could explain discrepancies between results. This part will be divided in three sections, each of them focused on a specific property. Each section will revisit the technique(s) used and show the most significant results.

European Commission | Horizon 2020 European Union funding for Research & Innovation

2 Full Database of Thermal Material Properties

Lining Zone	Materials		Temperature [°C]	Specific heat [J/(kg K)] (rule of mixtures)	Thermal conductivity [W/(m K)] (laser flash method)	Thermal expansion [%]	CTE [1 / K]
Working lining / slag zone	MgO-C bricks		800	1272		0.6*	$7.5 \cdot 10^{-6}$ (20 - 800 °C)
			1000	1296	7.5*		
			1200	1317		1.2*	
			1600	1345		1.7*	
Working lining / barrel zone	Alumina spinel bricks		800	1263	2.94		$8.8 \cdot 10^{-6}$ (30 - 1500 °C)
			1000	1293	2.66		
			1200	1318	2.41	1	
Safety Lining	Bauxite bricks		400	1124	2.8	0.3	$7.8 \cdot 10^{-6}$ (20 - 1200 °C)
			800	1204	2.5	0.6	
			1000	1214	2.3	0.8	
			1200	1253	2.0	0.9	
Insulating Lining	Insulating Boards	Low Density	400	1094	0.25	0.3	$9.1 \cdot 10^{-6}$ (20 - 700 °C)
			600	1132	0.26	0.5	
			900	1149	0.26	0.8	
		Medium Density	400	1094	0.28	0.3	$9.3 \cdot 10^{-6}$ (20 - 700 °C)
			600	1132	0.29	0.5	
			900	1149	0.26	0.8	
		High Density	400	1094	0.32	0.5	$10 \cdot 10^{-6}$ (20 - 700 °C)
			600	1132	0.33	0.6	
			900	1149	0.33	0.8	
Insulating Lining	Insulating Fireclay Bricks		400	1128	0.39	0.2	$6.4 \cdot 10^{-6}$ (20 - 570 °C)
			600	1182	0.39	0.3	
			800	1205	0.39	0.4	
			1000	1222	0.42	0.5	
			1200	1239	0.43	0.7	

*Data Sheet of RHI-Magnesita

European Commission | Horizon 2020 European Union funding for Research & Innovation

3 Specific heat

The specific heat capacity (Cp) represents the amount of heat energy necessary to increase the temperature of a substance by one degree Celsius. This property is related to the internal energy of a system, with lattice vibrations accounting for the majority of this internal energy in ceramic materials. For polycrystalline materials, the lattice can be described as an ordered structure of atoms, which vibrate around ideal equilibrium positions. As a result of this interconnected nature, the displacement of one atom from the equilibrium position leads to the stimulation of vibration waves [1][2].

An accurate measurement of this thermal property is often quite complicated. Therefore, two techniques were compared: Differential Scanning Calorimetry (experimental test) and the rule of mixtures (empirical formula).

Differential Scanning Calorimetry is a thermo-analytical technique in which the difference in the amount of heat required to increase the temperature of a sample and a reference is measured as a function of temperature. Both the sample and the reference are maintained at nearly the same temperature throughout the experiment. The reference sample should have a well-defined heat capacity over the range of temperatures to be scanned [3]. The basic principle underlying this technique is that when the sample undergoes a physical transformation, such as phase transitions, more or less heat will need to flow into it than into the reference to maintain both at the same temperature. Whether more or less heat must flow to the sample depends on whether the process is exothermic or endothermic [3]. For this method, the samples were ground and left 24h in an oven at 100 °C before the measurements were taken. The experiments were carried out up to the maximum temperature of interest. In the case of insulating materials, the measurements were made up to 1000 °C. For materials used in the working lining, a maximum temperature of 1500 °C was used. All materials were heated in a static air atmosphere, at a rate of 5 K/min, using sapphire as a reference. Furthermore, for each material, three tests were made to confirm the accuracy of the results (Figure 1).

The experimental results were then compared with the values obtained with the formula for the rule of mixtures (Equ. 1) [4]:

$$C_{\mathrm{p}} = \sum_{i} m_i C_{pi} \qquad \text{Equ. 1}$$

Where m_i is the percentage in mass of each compound and C_{pi} the specific heat of each of them [5]. The percentage can be evaluated using inductively coupled plasma mass spectrometry (ICP-MS) or X-ray fluorescence (XRF) analysis. Furthermore, the values of C_{pi} are temperature dependent, and thus Equ. 1 should be applied to each temperature. Figure 1 shows an example of the Cp curves obtained with the DSC method in the case of Low Density Insulating Boards. Medium and High Density Insulating Boards, also show the same trend. Furthermore in the graph, the values obtained with the rule of mixtures are also reported (black dots).

European Commission | Horizon 2020 European Union funding for Research & Innovation

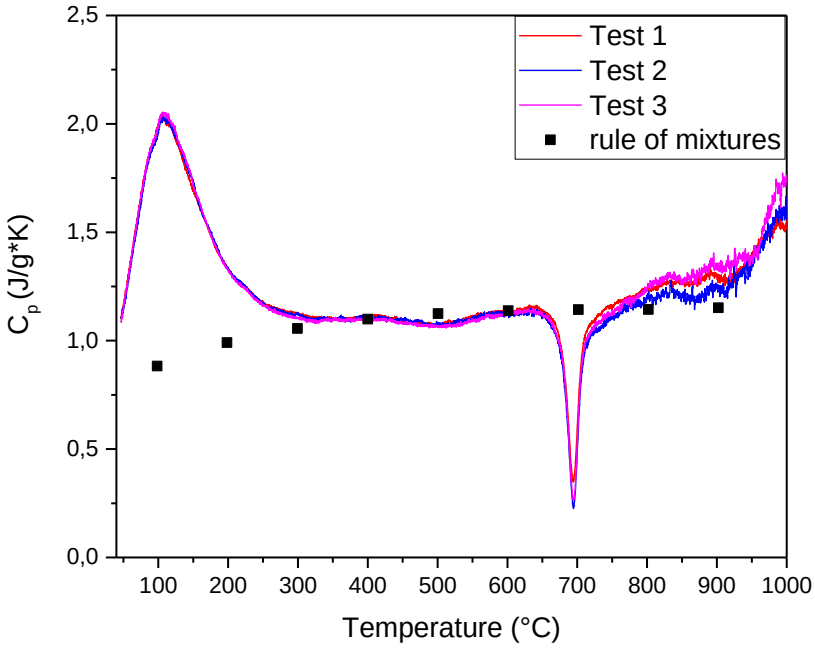

Figure 1: Differential Scanning Calorimetry results for Low Density Insulating Boards. The measurements were carried out up to 1000 °C in static air atmosphere.

The exothermic peak at ~ 110 °C in the DSC results (Figure 1) can be explained considering DTA (differential thermal analysis) measurements previously discussed in the literature. In the DTA graph, it is possible to observe an endothermic peak between 20 °C and around 250 °C. According to literature studies [6][7], the removal of the physically adsorbed water and the interlayer water residing in the particle space of the vermiculite, not in immediate contact with cations (in this case, Mg^{2+}), is observed in this temperature range. Thus, even if the samples were dried before the measurements, the chosen temperature (100 °C) was not sufficient to completely remove the interlayer water. Furthermore, the water has a specific heat of around 4.2 J/(g K) [5] at room temperature and thus, its presence increases the specific heat values of the refractory material (exothermic peak). In the empirical formula, the water molecules are not taken into account during the calculation. This explains why the values obtained by DSC are higher than the calculated values in the range 20 - 250 °C.

Above 250 °C, the two methods give a good agreement between the results (Figure 1). The difference is around 1 %. Only between 650 °C and 750°C, the values do not match perfectly due to the formation of a new amorphous phase (endothermic peak in Figure 1). The differences between the different experimental curves, which are more evident at temperatures > 800 °C, are mostly linked to slight discrepancies between samples [8].

Therefore, Equ. 1 was used to calculate the specific heat values for all the investigated materials. For each refractory material, some of the calculated values are shown in the section 2: “Full Database of Thermal Material Properties”.

4 Thermal conductivity

The thermal conductivity (λ) is the property that represents the ability of the material to propagate the heat, both in the solid and in the pore phases. It can be calculated using different techniques (most of which are described in Deliverable 1.3) [3] but this leads to some variations in the obtained values. In the ATHOR project, four methods were compared: the laser flash, the hot disk, the hot wire and the heat flow meter. A short reminder of these techniques will be given in this section.

4.1 A short reminder about the laser flash method

The laser flash method (Figure 2) is a transient method for the evaluation of the thermal diffusivity (α) of different materials developed by Parker et al. in 1961 [9]. From literature [10][11], this method is well adapted for thermal diffusivity values ranging between 0.1 and 1000 $mm^2\ s^{-1}$. The main advantages of using this technique are: i) simple specimen geometry, ii) rapidity of measurements, iii) no contact resistance between the sample and the heat source.

The principle consists of sending an energy pulse to impact the front face of a disk shaped sample. The absorbed heat diffuses throughout the material and the resulting time-dependent temperature on the opposite face is monitored by an infrared detector. The evaluation of α from this time-dependent temperature curve can be performed with different models. One model is that of

European Commission | Horizon 2020 European Union funding for Research & Innovation

Mehling, which takes into account (in addition to the heat losses during the experiment) radiation transfer between the front and back faces [12].

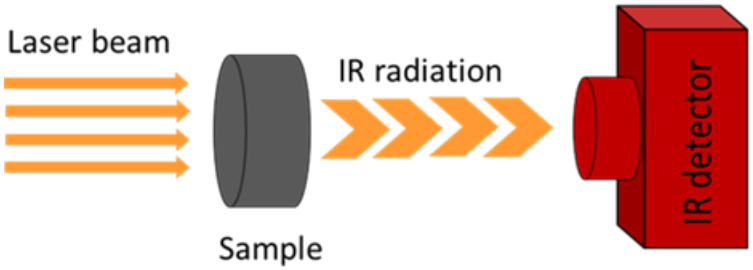

Figure 2: Schematic diagram of the laser flash method.

The thermal conductivity is then calculated using Equ. 2:

$$\lambda = \alpha \, \rho \, C_p \qquad \text{Equ. 2}$$

Where α is the thermal diffusivity, ρ the bulk density and Cp the specific heat capacity. For each investigated material, two samples were analysed and three measurements for each temperature were taken. High temperature measurements were made, under an argon atmosphere, on disk samples (diameter of 10 mm, thickness of 2 mm). All specimens were covered by a layer of graphite to increase the heat absorbed on the front face and the radiation emitted by the back face [13][14].

The uncertainty of this method is taken to be ± 5% at room temperature [10] and it can increase up to 10 - 15 % at high temperatures depending on the material and on the quality of the T-t curve, which can present noise due to the hot environment and radiation effects.

4.2 A short reminder about the hot disk method

The hot disk method is also known as the transient plane source (TPS), for the evaluation of the thermal conductivity and the thermal diffusivity of different materials. From literature [15][16], this method is well adapted for thermal conductivity values ranging between 0.005 and 500 W m^{-1} K^{-1}. The main advantages are: i) short measurement times, ii) easy sample preparation, iii) different sensor sizes to accommodate different sample types, iv) non-destructive.

The TPS sensor is a double nickel spiral, supported by two thin sheets of an insulting material (kapton, mica or teflon), placed between two halves of the same material (Figure 3). This sensor has a double function: as a heat source for increasing the temperature of the materials and as a “resistance thermometer” for recording the temperature increase as a function of time. Certain parameters are required to be clearly defined in accordance with the material under investigation: the radius of the probe (depending on the dimensions of the sample); the type of sensor (depending on the temperature range to measure); the heating power (to have a temperature increment of 2-5 K); the measurement time (for recording n-points and having a total characteristic time of at least 0.4 s). All these parameters should be chosen to guarantee a maximum probing depth, which is less than the minimum distance between the sensor and the borders of the sample, in radial and axial directions. This is very important because the theory (behind the analytical formula used to make the evaluation) considers the sample as an infinite medium. In addition, a perfect contact is assumed between the sensor and the two sample surfaces in contact with it. In fact, because this is not exactly true, the initial data points are excluded from the analysis for evaluation of the thermal properties [17][14].

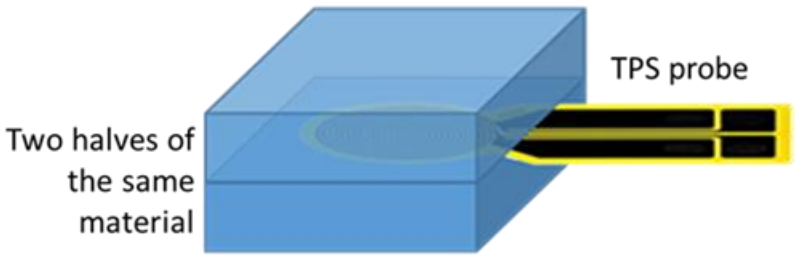

Figure 3: Schematic diagram of the hot disk method.

In case of isotropic materials, the calculation of the thermal conductivity requires a value for the temperature increase of the sample surface facing the TPS sensor (ΔT_s). To obtain this value, an iteration procedure, which gives the thermal diffusivity as an optimum variable, is first carried out. This iteration establishes a linear relationship between the temperature increase ΔT and

European Commission | Horizon 2020 European Union funding for Research & Innovation

the dimensionless specific time function $D(\tau)$. ΔT_s is then obtained from the resulting slope enabling the calculation of the thermal conductivity using Equ. 3:

$$\Delta T_s(\tau) = P_0 \left(\pi^{\frac{3}{2}} r \lambda\right)^{-1} D(\tau) \qquad \text{Equ. 3}$$

Where $\Delta T_s(\tau)$ is the increase in temperature of the two surfaces in contact with the probe, $D(\tau)$ the dimensionless specific time function, P_0 is the heating power and r the radius of the probe.

In the case of anisotropic materials, the procedure is quite similar. One important parameter, which must be chosen at the beginning of the measurements, is the specific heat for unit volume ($\rho \cdot C_p$). This value must be correct or the ratio between axial and radial results would be false [15]. The iteration gives, as an optimum variable, the radial thermal diffusivity (α_{rad}) and the radial thermal conductivity (λ_{rad}) is calculated using Equ. 2. Then, the axial thermal conductivity (λ_{ax}) is given by:

$$\Delta T_s(\tau_{rad}) = P_0 \left(\pi^{\frac{3}{2}} r \lambda_{rad} \lambda_{ax}\right)^{-1} D(\tau_{rad}) \qquad \text{Equ. 4}$$

And the axial thermal diffusivity (α_{ax}) is obtained by Equ. 2.

The measurements were made at room temperature, in an air atmosphere and under a cover to keep the experimental conditions stable. For each material, three couples of square samples were analysed. Typical dimensions: 70 x 70 cm^2 and 25 - 35 mm thick.

The uncertainty of this method is estimated to be 2 - 5% for the thermal conductivity and 5 - 10 % for the thermal diffusivity [15].

4.3 A short reminder about the hot wire method

The hot wire method (Figure 4) is a transient method often used for the determination of the thermal conductivity of refractory materials (λ < 15 W m^{-1} K^{-1}) [18]. Several configurations of this technique are available. In the ATHOR project, the parallel method was used [19][20]. For each measurement, three samples are needed. The wire is placed between the sample at the bottom and the sample in the centre and a thermocouple is placed parallel to the (heating) wire at a specific distance (r = 15 mm). A reference thermocouple is placed between the sample in the centre and the sample of the top in an orthogonal direction compared to the previous one. The theory is quite similar to the hot disk method. The difference is that, in this case, the heat source is a platinum wire, which is assumed to be infinitely thin and long and surrounded by an infinite medium. When a constant electrical current is applied, a constant amount of heat flux is generated all along the wire and this causes a transient temperature field, logarithmically dependant on time. The non-linearity at the beginning (from t = 0 to t_{min}) is due to the contact resistance between the samples and the wire, while the non-linearity at the end (t > t_{max}) is due to the finite dimensions of the samples [14].

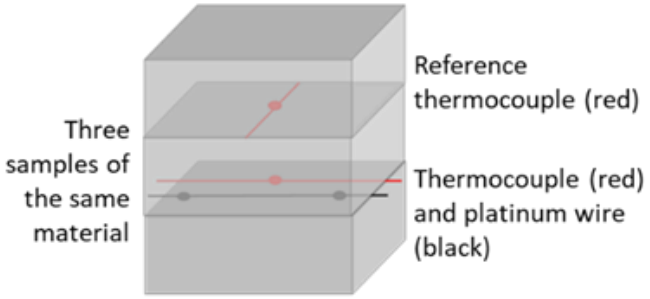

Figure 4: Schematic diagram of the hot wire method.

The thermal conductivity is calculated using Equ. 5:

$$\lambda = -\frac{q}{4\pi\, T(t)} E_i\left(\frac{-r^2}{4\,\alpha\, t}\right) \qquad \text{Equ. 5}$$

Where q is the heat flow, α the thermal diffusivity, r the distance between the wire and the thermocouple, T(t) the temperature rise compared to the reference temperature and t the time to reach that temperature. For each measurement, three samples were used (250 x 114 x 50 mm^3). Furthermore, the measurements were carried out in air atmosphere between 200 °C and the maximum temperature of interest.

The uncertainty of this method is taken to be ± 6 % for small power levels and ± 1 % for high power levels [21].

European Commission | Horizon 2020 European Union funding for Research & Innovation

4.4 A short reminder about the heat flow meter

The heat flow meter (Figure 5) is a steady-state method for the determination of the thermal conductivity of insulating material ($\lambda < 1$ W m^{-1} K^{-1}) at ambient conditions [11][22]. As for all the steady-state techniques, it requires a long measurement time. For instance, for the materials investigated in the following report, it took between 40 and 60 minutes to reach the equilibrium.

The sample is placed between two thin copper plates equipped with thermocouples and heat flow sensors. In the top plate, an electrical resistance is also embedded to work as a heat source. The power dissipation is chosen in order to have a temperature difference of around 4 °C between the two faces of the sample.

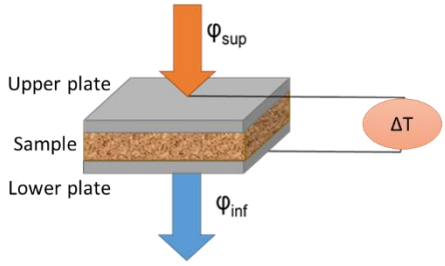

Figure 5: Schematic diagram of the heat flow meter.

The technique then measures the apparent thermal resistance as:

$$R_{app} = \frac{\Delta T}{(\varphi_{sup} + \varphi_{\inf})/2} \qquad \text{Equ. 6}$$

Where φ_{sup} is the heat flow supplied to the sample, φ_{inf} is the heat flow coming out from the sample and ΔT the gradient of temperature between the two plates. The results are plotted as a function of the thickness resulting in a linear relationship. The thermal conductivity is given by the inverse of the slope. For each material, between four and six samples were analysed with different thicknesses (from 2 to 15 mm) and surface area of 30 x 30 mm^2. The measurements were made in an air atmosphere at room temperature.

The uncertainty of this method is estimated to be ± 3 % [23].

4.5 Comparison of the experimental values

Table 1 shows an example of results for the Insulating Fireclay Bricks (insulating materials with a homogenous microstructure at the macroscopic level), High Density Insulating Boards (insulating material with a heterogeneous microstructure) and Alumina Spinel Bricks (conducting material with a heterogeneous microstructure) at room temperature. Three methods are compared: laser flash (LFA), hot disk (TPS) and heat flow meter (HFM). Room temperature measurements are not available in the case of the hot wire method (HWM) because the time to achieve the equilibrium temperature distribution inside the material was too long. Therefore, the accuracy of the results at T < 200 °C was considered insufficient. The heat flow meter was not used in the case of Alumina spinel brick because, as written in the paragraph 4.4, this technique measures the thermal conductivity of materials with $\lambda < 1$ W m^{-1} K^{-1}. It is important to underline that the Insulating Boards are anisotropic materials, and thus at least two directions should be investigated. In the case of the laser flash method, the anisotropic behaviour was investigated by cutting disk samples in two different directions. In contrast, in the case of the hot disk method, no change in the sample configuration was necessary but an anisotropic software module was used. Finally, in the case of the heat flow meter, it was not possible to take into account this aspect because there was insufficient volume available for cutting samples in different directions. In Table 1, only the values in the pressing direction are reported for the three refractory materials. This is the most important direction for steel ladle applications. The main purposes of the three linings of refractories (the working lining, the safety lining and the insulating lining) consist of: i) protecting against corrosion and erosion, ii) avoiding infiltration, iii) acting as a physical barrier between the hot medium and the wall of the vessel, and iv) providing thermal insulation. Therefore, knowing the thermal properties through the thickness of the vessel (cross-plane direction) allows to: i) maintain the temperature of the bath above the casting temperature, ii) save energy consumption, iii) reduce energy costs and environmental impacts

European Commission | Horizon 2020 European Union funding for Research & Innovation

Table 1: Thermal conductivity values for the high-density insulating boards, insulating fireclay bricks and alumina spinel bricks at room temperature, using three different methods.

Material	LFA λ (W m^{-1} K^{-1})	TPS λ (W m^{-1} K^{-1})	HFM λ (W m^{-1} K^{-1})
Insulating Fireclay Bricks	0.36 ± 3.5%	0.38 ± 3.9%	0.45 ± 3%
High Density Insulating Boards	0.27 ± 1.5%	0.43 ± 1%	0.36 ± 3%
Alumina spinel bricks	6.5 ± 1.7%	5.3 ± 1%	-

The table shows that the each set of results is reproducible. The standard deviations are, in fact, between 1.5 % and 3.5 % in the case of the laser flash method, between 1 % and 4 % in the case of the hot disk method and 3 % for the heat flow meter. On the other hand, it also shows that the three methods give quite different results with a higher discrepancy in the case of the insulating board. It is important to underline that each technique does not probe the material in the same heat flow direction, asses the thermal conductivity over the same sample volume or in identically experimentally conditions. As a consequence, the information obtained with one method does not compare directly to that given by another technique.

Firstly, the heat flow meter and the laser flash have similar heat flow directions (linear in both cases). In the case of the hot disk method, the heat flow is spherically radial to the disc probe shape, while in the case of the hot wire method it is radial to the wire. Secondly, the laser flash is made in an argon atmosphere, which is reached after three cycles of vacuum followed by argon flow. Therefore, the samples could be considered as being dried before the laser flash measurements. While in the case of the heat flow meter and the hot disk method, the measurements are made in an air atmosphere with a typical relative humidity of 50 %. In the case of the hot wire method, humidity is not an important parameter since the tests are made starting from 200 °C. Finally, the hot disk and hot wire methods use larger samples, which can give a more accurate average value of thermal conductivity in the case of heterogeneous materials. Thus, it is not possible to compare the results obtained with the different methods if some modifications to have equivalent conditions are not made.

Depending on the type of material investigated and on the technique used, factors such as heat loss and humidity were taken into account in order to correct the experimental results in similar experimental conditions (Table 2). For instance, in the case of HFM, lateral heat losses play an important role. They can be considered as a parallel thermal resistance, which reduces the overall thermal resistance (R) and consequently, it increases the thermal conductivity ($\lambda = 1/R$). Thus, if they are not taken into account, the experimental results would be higher that the real values. For this purpose, a heat sink term (P) was introduced in the one-dimensional steady-state heat equation [24]:

$$\frac{d^2T}{dz^2} + \frac{P}{\lambda} = 0 \qquad \text{Equ. 7}$$

Where λ is the thermal conductivity calculated on samples with thicknesses less than 6 mm. This value was chosen using the approximation that for small thickness, the later heat losses are negligible. By combining Equ. 7 with Fourier's law in one dimension:

$$\varphi(z) = -\lambda \frac{dT}{dz} \qquad \text{Equ. 8}$$

The incoming and outgoing heat flows, as well as the upper and lower temperatures, were re-calculated and introduced in Equ. 6 for obtained the new apparent thermal resistance. The heat losses are also important in the case of LFA. However, by building the good model in the LFA software (Mehling in this case), they were already taken into account in the obtained experimental results.

If the material is particularly sensitive to its thermal and hydric history (as in the case of the insulating boards), the TPS and HFM will give a higher value if the samples are not previously dried. This is because the air in the pores (0.026 W m^{-1} K^{-1}) is replaced by water (0.6 W m^{-1} K^{-1}). Therefore, the measurements were made on samples, which were left for 24h in an oven at 200 °C. This temperature was chosen to be sure to remove the physical adsorbed water and the interlayer water (see the paragraph about the specific heat). The same experimental conditions were used for the insulating fireclay bricks and the alumina spinel bricks, but no significant effects were observed.

Table 2 shows the results after the correction taking into account heat losses and humidity effects.

European Commission | Horizon 2020 European Union funding for Research & Innovation

Table 2: Thermal conductivity values for the high density insulating boards, insulating fireclay bricks and alumina spinel bricks at room temperature, using three different methods. Corrections were made to obtain similar experimental conditions.

Material	LFA λ (W m^{-1} K^{-1})	TPS λ (W m^{-1} K^{-1})	HFM λ (W m^{-1} K^{-1})
Insulating Fireclay Bricks	0.36 ± 3.5%	0.38 ± 3.9%	0.40 ± 3%
High Density Insulating Boards	0.27 ± 1.5%	0.34 ± 1%	0.26 ± 3%
Alumina spinel bricks	6.5 ± 1.7%	5.3 ± 1%	-

This table shows that it is possible to achieve a good agreement between the techniques, with maximum discrepancy within 10 % in the case of the insulating fireclay bricks. In the case of the alumina spinel bricks, the difference is around 20 % even if the material is isotropic as the previous case. This might be linked to the heterogeneous nature of the refractory. Furthermore, in the case of the insulating boards, it is possible to observe a good agreement between the HFM and the LFA (discrepancy within 10 %), while the TPS gives a higher value (discrepancy within 26 %). This might be linked to the anisotropic behaviour of the refractory, but also to different heat flow directions.

Another aspect to consider is the type of information that each technique gives. The hot wire method, for instance, gives an average value of the thermal conductivity over the different heat flow directions (Figure 6). Therefore, in the case of anisotropic materials, it is less suitable. Furthermore, if the values obtained with the HWM in the case of anisotropic materials are used as input parameters for modelling studies, the thickness of the insulating lining will be overestimated causing economic problems.

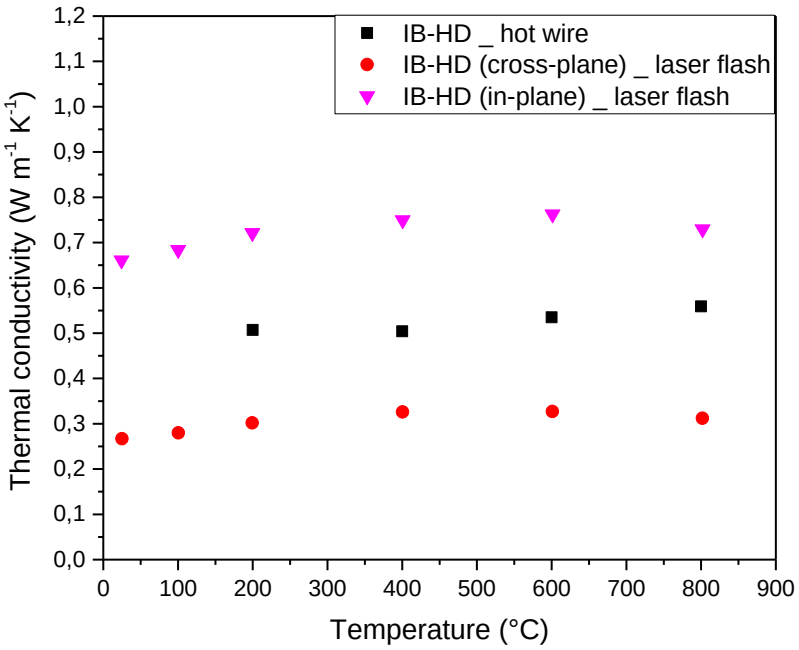

Figure 6: Comparison between the hot wire and the laser flash methods in the case of an anisotropic materials (High Density Insulating Boards).

The graph shows that the results obtained with the hot wire method are in between of those obtained with the laser flash method in the two directions: cross-plane, pressing direction; and in-plane, against pressing direction.

For input parameters in the simulation models, the data obtained with the laser flash method is most appropriate in cross plane direction, since it provides a direct value of λ without any need for correction. In addition, this technique allows values of thermal conductivity to be recorded over a greater temperature range. For each refractory material, some of the experimental results are shown in the section 2: “Full Database of Thermal Material Properties”.

5 Thermal expansion

Thermal expansion shows the tendency of a material to change its volume or its dimensions due to a change of temperature. This is linked to atomic vibrations and asymmetry in the interatomic pair potential. With the increase in temperature, the atoms start to move with higher amplitude increasing the interatomic distance. These changes are normally small but of great

European Commission | Horizon 2020 European Union funding for Research & Innovation

importance. Refractories are a mixture of two of more solid phases. If each phase has a different coefficient of thermal expansion, the induced mismatch will cause the formation of micro-cracking within the microstructure. This diffuse damage can be beneficial for resistance to thermal shock because it favours the reduction of the overall thermal expansion, although it can sometimes lead to rupture.

5.1 Dilatometry

Dilatometry measurements yield precise information on dimensional changes, such as expansion or shrinkage, during a heating/cooling cycle. The measurement is based on a pushrod technique, dimensional changes are detected by the displacement system. This displacement system is connected to the sample, undergoing microstructural changes, via a pushrod. For an accurate determination, it is necessary to calibrate the equipment by using a reference material (generally alumina) that has a known and reproducible thermal expansion [3]. The equipment measures the change in length as a function of temperature, and the linear coefficient of thermal expansion (CTE) is then calculated with Equ. 9:

$$CTE = \frac{1}{L_o}\frac{\Delta L}{\Delta T} \qquad \text{Equ. 9}$$

where L_0 is the initial length of the sample.

Thermal expansion values maybe influenced by multiple factors such as material anisotropy, thermal history e.g. the firing temperature and duration, repeated firing and measurement conditions like atmosphere, pressure and heating rate. Figure 7 illustrates the influence of the heating rate on the thermal expansion coefficient, in the case of a sintered polycrystalline alumina-rich spinel ($MgAl_2O_4$) and an alumina-spinel fired brick. A difference in the CTE (30 - 1500 °C) determined at different heating rates can be observed for both materials containing alumina-rich spinel. Such a discrepancy in the thermal expansion behaviour may be associated with precipitation / dissolution phenomena (related to the equilibrium between a spinel solid solution containing a variable Al_2O_3 / MgO ratio and pure Al_2O_3), where such precipitation / dissolution of alumina causes additional linear changes. A fact, that thermal expansion behaviour can be influenced by heating rate, that has been barely reported in the literature and is frequently ignored in numerous investigations. Nevertheless, as reported here, heating rate may be an additional, important factor which affects the thermal expansion behaviour of spinel containing refractory materials ($MgAl_2O_4$).

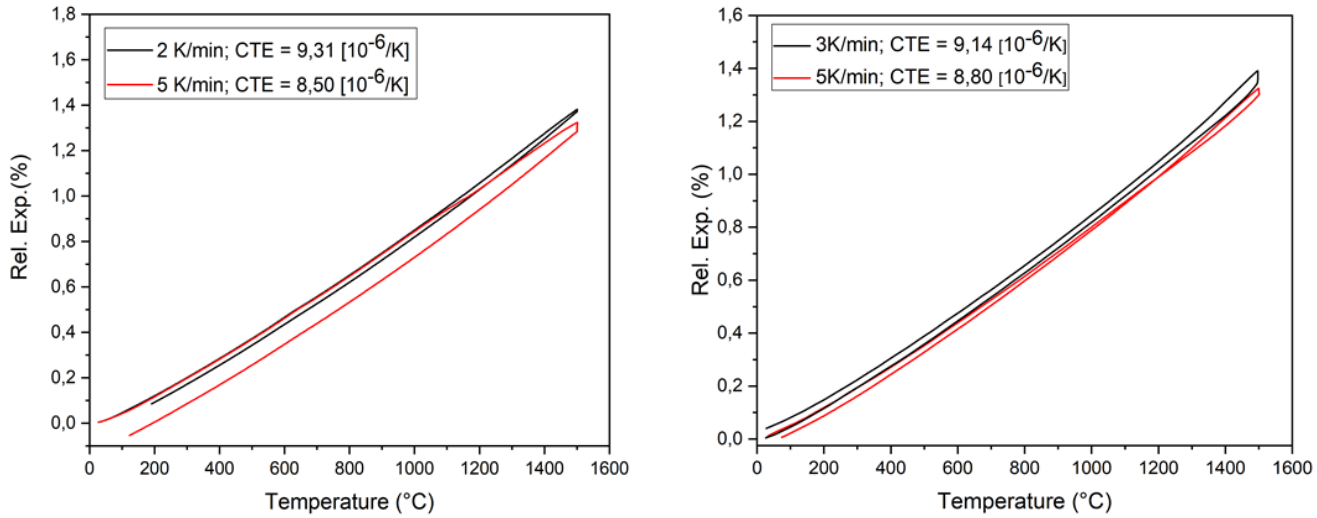

(a) (b)

Figure 7: Relative expansion ($\Delta L / L_o$) versus temperature with calculated $CTE_{(30-1500°C)}$ determined at different heating rates for samples of: a) sintered polycrystalline alumina-rich spinel, and, b) alumina-spinel fired brick.

5.2 Refractoriness Under Load / Creep In Compression (RUL/CIC)

Thermal expansion can be measured alternatively by Refractoriness Under Load / Creep In Compression (RUL/CIC) apparatus described previously in greater detail [1]. This measurement technique allows for measurement of bigger samples (cylindrical test piece: 50 mm in diameter and height with coaxial bore of 12.5 mm) compared to standard dilatometry test pieces (rectangular shape: 5 x 5 x 25 mm^3). Thus RUL/CIC may be advantageous for materials containing bigger aggregates such as refractories or when influence of additional factors (load) will be investigated. Figure 8 shows the influence of thermal shock on thermal expansion

European Commission | Horizon 2020 European Union funding for Research & Innovation

characteristics of alumina-spinel brick obtained with RUL/CIC apparatus. This investigation was conducted to prove the hypothesis that the material damage caused by thermal shock triggers sintering phenomena and this is more and more significant with the advancement of damage. From the thermodynamic point of view, the driving force for sintering comes from the high surface energy and the surface curvature. Once sintering starts, surface energy is consumed through particle bonding, resulting in an increased strength and often a dimensional change. Therefore, thermal hysteresis curves, generated by dilatometry, can be used to monitor and estimate the degree of such re-sintering and crack-healing phenomena. Microstructure of materials exposed to thermal cycling conditions is characterized by the presence of micro-cracks and thermal strains/stresses accommodated in the material. With the progress of material damage, the length and density of cracks increase and complex state of stress develops, resulting in an increased system energy. At this stage (after thermal shock), the microstructure of the damaged material can be equated with the microstructure of the material at the early stages of sintering, characterized by a high surface energy. The natural tendency of the system is to reduce its energy, therefore at high temperature, various mass transport mechanisms are activated to move particles from convex to concave surfaces. In the conducted experiments, material shrinkage was observed after a second thermal shock, which indicates that damage induced by two thermal shocks, triggered re-sintering and crack-healing phenomena. This phenomenon was not observed after the first thermal shock, which may indicate that level of material damage at this stage was not sufficient to induce mass transport phenomena.

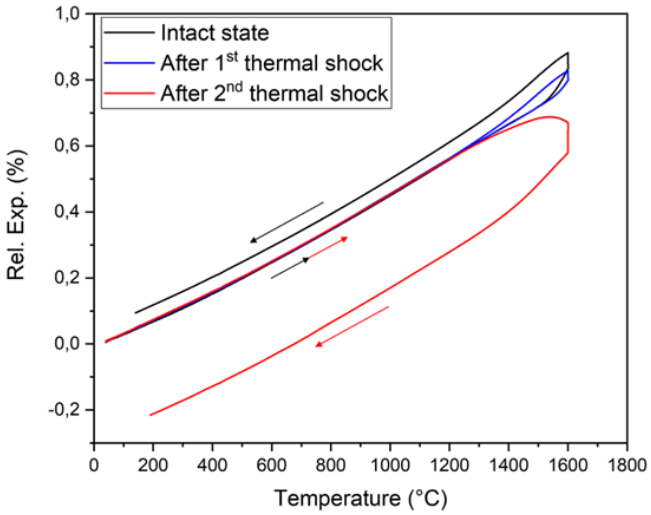

Figure 8: Influence of thermal shocks on the relative thermal expansion ($\Delta L / L_o$) in the case of an alumina-spinel fired brick.

6 Conclusion

Thermal properties are very important input parameters for modelling studies. Considering that they can evolve with temperature and microstructure, it is fundamental to understand this evolution to avoid serious working accidents.

In this deliverable, three main properties were analysed:

- specific heat;
- thermal conductivity;
- thermal expansion.

The specific heat is the amount of heat energy necessary to increase the temperature of a substance by one degree Celsius. It is not always easy to have an accurate value in the temperature range which is of industrial interest. However, it was demonstrated that the rule of mixtures works very well for this purpose. The comparison between the Differential Scanning Calorimetry and the rule of mixtures, in fact, exhibits a difference of 1 % in the temperature range 200 - 900 °C.

The thermal conductivity is the ability of the material to propagate the heat, both in the solid and in the pore phases. It can be measured with different techniques, which lead to some variations in the obtained values. However, taking into account some parameters such as heat losses and humidity, the maximum discrepancy could be reduced within 10 % when the same heat flow direction through the material is considered. Heterogeneity and anisotropy are other factors to take into account to better interpret the results.

The thermal expansion is the tendency of a material to change its volume or its dimensions due to a change of temperature. Normally, the coefficient of linear expansion is estimated by dilatometry measurements. However, the RUL/CIC apparatus may

European Commission | Horizon 2020 European Union funding for Research & Innovation

give comparable results and, additionally, could be advantageous for materials containing bigger aggregates (such as refractories) or when the influence of additional factors (load) should be investigated.

7 References

[1] D. Cahill and R. O. Pohl, "Lattice Vibrations And Heat Transport In Crystals And Glasses," *Annu. Rev. Phys. Chem.*, vol. 39, no. 1, pp. 93–121, 1988.

[2] P. G. Klemens, "Heat conduction in solids by phonons," *Thermochim. Acta*, vol. 218, pp. 247–255, 1993.

[3] D. Vitiello, I. Kieliba, G. Derrick, and M. Huger, "Deliverable D1.3: Devices for Thermo-Physical Properties Characterisation," 2019.

[4] D. Günther and F. Steimle, "Mixing rules for the specific heat capacities of several HFC-mixtures," *Int. J. Refrig.*, vol. 20, no. 4, pp. 235–243, 1997.

[5] O. Knacke, O. Kubaschewski, and K. Hesselmann, *Thermal Chemical Properties of Inorganic Substances*, 2nd Ed. Springer Verlag, 1977.

[6] L. A. Pérez-Maqueda *et al.*, "Study of natural and ion exchanged vermiculite by emanation thermal analysis, TG, DTA and XRD," *J. Therm. Anal. Calorim.*, vol. 71, no. 3, pp. 715–726, 2003.

[7] P. Kresten and G. Berggren, "The thermal decomposition of vermiculite," *Thermochim. Acta*, vol. 23, pp. 171–182, 1978.

[8] G. Della Gatta, M. J. Richardson, S. M. Sarge, and S. Stolen, "Standards, calibration, and guidelines in microcalorimetry. Part 2. Calibration for differential scanning calorimetry (IUPAC Technical Report)," *Pure Appl. Chem.*, vol. 78, no. 7, pp. 1455–1476, 2006.

[9] W. J. Parker, R. J. Jenkins, C. P. Butler, and G. L. Abbott, "Flash method of determining thermal diffusivity, heat capacity, and thermal conductivity," *J. Appl. Phys.*, vol. 32, no. 9, pp. 1679–1684, 1961.

[10] ASTM International, "Standard Test Method for Thermal Diffusivity by the Flash Method 1," *ASTM Int.*, vol. E1461-13, pp. 1–11, 2013.

[11] H. Czichos, T. Saito, and L. Smith, Eds., *Springer Handbook of Metrology and Testing*, 2nd editio. Springer, 2011.

[12] H. Mehling, G. Hautzinger, O. Nilsson, J. Fricke, R. Hofmann, and O. Hahn, "Thermal diffusivity of semitransparent materials determined by flash laser method applying a new analytical model," *Int. J. Thermophys.*, vol. 19, no. 3, pp. 941–949, 1998.

[13] A. P. F. Albers, T. A. G. Restivo, L. Pagano, and J. B. Baldo, "Effect of testing conditions on the laser flash thermal diffusivity measurements of ceramics," *Thermochim. Acta*, vol. 370, no. 1–2, pp. 111–118, 2001.

[14] T. Tonnesen, R. Telle, D. S. Smith, and S. Fayette, "A modified equipment for determination of thermal conductivity of refractories by the hot-wire method-a critical review and comparison with the laser-flash-method," in *UNITECR 1999*, 1999, pp. 416–420.

[15] ISO Standard, "Plastic - Determination of thermal conductivity and thermal diffusivity - Part 2: Transient plane source method," *ISO 22007-22008*, pp. 1–24, 2008.

[16] "Hot Disk Thermal Constants Analyser: Instruction Manual." Hot Disk AB, pp. 1–128, 2015.

[17] S. E. Gustafsson, "Transient plane source techniques for thermal conductivity and thermal diffusivity measurements of solid materials," *Rev. Sci. Instrum.*, vol. 62, no. 3, pp. 797–804, 1991.

[18] J. Boer, J. Butter, B. Grosskopf, and P. Jeschke, "Hot wire technique for determining high thermal conductivities," *Refract. J.*, pp. 22–28, 1980.

[19] W. N. Dos Santos and R. Gregorio, "Hot-wire parallel technique: A new method for simultaneous determination of thermal properties of polymers," *J. Appl. Polym. Sci.*, vol. 85, no. 8, pp. 1779–1786, 2002.

[20] J. J. Healy and J. J. De Groot, "The theory of the transient hot-wire method for measuring thermal conductivity," *Physica*, vol. 82C, pp. 392–408, 1976.

[21] U. Hammerschmidt and W. Sabuga, "Transient hot wire (THW) method: Uncertainty assessment," *Int. J. Thermophys.*, vol. 21, no. 6, pp. 1255–1278, 2000.

[22] J. Bourret, E. Prud'Homme, S. Rossignol, and D. S. Smith, "Thermal conductivity of geomaterial foams based on silica fume," *J. Mater. Sci.*, vol. 47, no. 1, pp. 391–396, 2012.

[23] ISO Standard, "Thermal insulation - Determination of steady-state thermal resistance and related properties - Heat flow meter apparatus," *ISO 8301-1991*, 2010.

[24] M. Trojan, "O: One-dimensional analytical models of frictional heating during braking," in *Encyclopedia of Thermal Stresses*, 2014.

European Commission | Horizon 2020 European Union funding for Research & Innovation